

Multiscale Modeling Approach to determine Effective Lithium-Ion Transport Properties

Harikesh Arunachalam*, *Student Member, IEEE*, Svyatoslav Korneev, Ilenia Battiato, and Simona Onori, *Senior Member, IEEE*

Abstract—This paper elaborates upon the limitations of using volume-averaged macroscale electrochemical models for lithium-ion batteries, such as the Pseudo-two-Dimensional (P2D) model [1]. To address some of these limitations, an enhanced electrochemical modeling framework that is developed using the homogenization technique is presented in this work. The mass and charge transport equations of the new modeling framework are derived by multiple-scale asymptotic expansion of the pore-scale Poisson-Nernst-Planck (PNP) equations [2]. The effective diffusion and conductivity coefficients of the homogenized model are determined by formulating and solving a closure variable in the electrode microstructure. This paper demonstrates the methodology to calculate the effective transport parameters using the closure approach. We compare the closure-based effective parameters with the effective parameters obtained by using the Bruggeman theory. The Bruggeman approach relies on a simplified approximation of the pore-scale parameters to determine effective values using only porosity. Results indicate that the Bruggeman approach underpredicts the effective transport parameters. This could critically influence model predictive ability, particularly for high C-rates and temperatures of battery operation.

NOMENCLATURE

| | |
|--------------------------|--|
| a_j | Electrode specific surface area [m^2m^{-3}] |
| $c_{s,j}$ | Pore-scale electrode concentration [$molm^{-3}$] |
| $c_{s,surf}$ | Electrode surface concentration [$molm^{-3}$] |
| $c_{s,max}$ | Electrode saturation concentration [$molm^{-3}$] |
| $\bar{c}_{s,j}$ | Average electrode concentration [$molm^{-3}$] |
| $\bar{c}_{e,j}$ | Average electrolyte concentration [$molm^{-3}$] |
| $\bar{\phi}_{s,j}$ | Average electrode potential [V] |
| $\bar{\phi}_{e,j}$ | Average electrolyte potential [V] |
| $\eta_{e,j}$ | Electrolyte volume fraction [–] |
| ε | Scale separation parameter [–] |
| \mathcal{K}^* | Dimensionless effective reaction rate constant [–] |
| $\mathbf{D}_{s,j}^{eff}$ | Effective electrode diffusion tensor [m^2s^{-1}] |
| $\mathbf{K}_{s,j}^{eff}$ | Effective electrode conductivity tensor [$S^{-1}m^{-1}$] |
| $\mathbf{D}_{e,j}^{eff}$ | Effective electrolyte diffusion tensor [m^2s^{-1}] |
| $\mathbf{K}_{e,j}^{eff}$ | Effective electrolyte conductivity tensor [$S^{-1}m^{-1}$] |
| $J_{Li,j}$ | Intercalation current density [Am^{-3}] |
| k_j | Interface reaction rate constant [$Ammol^{-1}$] |
| U_0 | Electrode open-circuit potential [V] |
| λ | A function of the activity coefficient [–] |
| t_+ | Transference number [–] |

H. Arunachalam and S. Onori are with the Department of Automotive Engineering, Clemson University, Greenville, SC, 29607, USA harunac@clemson.edu, sonori@clemson.edu

S. Korneev and I. Battiato are with the Department of Energy Resources Engineering, Stanford University, Stanford, CA 94305, USA skorneev@stanford.edu, ibattiato@stanford.edu

* corresponding author

| | |
|-----|--|
| F | Faraday's constant [$Asmol^{-1}$] |
| R | Universal gas constant [$Jmol^{-1}K^{-1}$] |
| T | Temperature [K] |

I. INTRODUCTION

Comprehensive understanding of the behavior of lithium-ion battery has remained a complex problem over decades. The challenge of this task is given by the nonlinearity of battery transport processes and heterogeneities that span across multiple length scales (*atomic to system*). Enhanced computational capabilities in recent years have been instrumental in the development of multiscale approaches to model the electrochemistry of lithium-ion batteries [3]. Pore-scale models incorporate microstructural details, but their computational intensity has led to the development of relatively simpler and efficient macroscale models [4]. For multiscale modeling of porous media, two approaches have been used to develop macroscale models from pore-scale governing equations: volume averaging [5] and homogenization [6].

In the volume-averaging technique, the variable of interest is first averaged over a representative elementary volume (REV) [5]. The REV is assumed to be a continuum representation of the underlying porous media. The pore-scale governing equations are then averaged in the REV so that they co-exist everywhere in the porous medium. Despite its implementation, the underlying approximations that form the basis of this approach have not been fully justified [5].

The homogenization technique uses asymptotic expansion of variables to determine the effective formulation of the governing equations as the pore-scale asymptotically approaches to zero [6]. This technique is more rigorous than volume-averaging, and is considered a multiscale modeling approach because it retains coupling between the pore-scale and the macroscale. The advantage of using homogenization over volume-averaging is that the resulting closure variables for effective transport parameters in the homogenized model are obtained by detailed numerical modeling of the electrode architecture, rather than using analytical approaches based on simplified assumptions [6].

The most commonly used macroscale electrochemical model to predict battery dynamics was developed by Doyle *et. al.* using the volume averaging technique [1], [5]. It is also called the pseudo two-dimensional (P2D) model because: a) it assumes spherical particles and resolves electrode mass transport in spherical coordinates, and b) it resolves electrode charge transport and electrolyte transport in 1-D cartesian coordinates. There are multiple limitations of

the P2D model in terms of: a) C-rate, b) temperature of operation, and c) prediction of the remaining useful life. Case study analyses presented in [7] identified that electrolyte mass transport limitations lead to diffusion limited regimes at high C-rates and invalidates classical macroscopic models. The study of temperature-influenced behavior of different battery electrodes in [8] revealed that classical macroscopic models may fail to predict battery dynamics beyond critical operating temperature conditions. Different studies [2], [4], [9] have reported that the P2D model is not robust enough to predict battery dynamics and failure mechanisms over the entire battery life.

These limitations have a critical impact on the accuracy of state-of-charge (SoC) and state-of-health (SoH) estimation. Simplified [10] and reduced-order models [11] for control-oriented applications are developed from the P2D model; hence their predictive ability at best is limited to the accuracy of the P2D model. In addition, model-based control strategies [12] to maintain a safe envelope of battery operation would clearly limit their threshold of application to only those conditions for which the underlying model is accurate. This may restrict the battery to only low C-rates of discharge and moderate temperatures of operation.

A major factor contributing to the limitations of the P2D model is the use of the Bruggeman theory to calculate effective diffusion and conductivity coefficients without considering the underlying microstructure [13]. Our motivation to pursue this research is to address some of the limitations of volume-averaged macroscale models using a homogenized macroscale modeling framework. In this paper, we elaborate upon the approach to determine the effective transport parameters of the mass and charge transport equations of the homogenized model. These effective transport parameters, determined using electrode microstructural information, are compared with the effective parameters of the P2D model. The P2D model effective parameters are obtained using the Bruggeman theory. We discuss the factors that are critical to obtain higher model-predictive ability, particularly for aggressive battery operating conditions.

This paper is structured as follows: In Section II, we conduct a comparative analysis of the new class of homogeneous macroscopic model equations with the classical P2D model, and emphasize upon the factors that indicate better predictive ability of the homogenized model over its volume averaged counterpart. In Section III, we emphasize the importance of the closure variable for determining effective transport parameters. In IV, we present the methodology to calculate the effective diffusion and conductivity tensors using the computational fluid dynamics (CFD) solver OpenFOAM [14]. Section V summarizes the conclusions of this work.

II. HOMOGENIZED EQUATIONS AND COMPARATIVE ANALYSIS

In this section, we discuss similarities and differences between the mass and charge transport governing equations of the P2D model, obtained from [15], and the homogenized model proposed in this work. The homogenization approach

considers the porous medium of the lithium-ion battery to be composed of spatially periodic unit cells Y . Each unit cell consists of multiple active electrode particles that are surrounded by the electrolyte. The electrode and electrolyte phases are separated by an interface where the reaction mechanism takes place. For a detailed description and derivation of the homogenized model equations, we refer the reader to [7]. Table I presents the transport equations of the P2D model and the homogenized model, and the intercalation current density.

A. Mass transport in the electrode

Fick's law of diffusion is used to define the governing equation for electrode mass transport. The P2D model assumes spherical particle shape for electrode concentration dynamics. The electrode concentration is represented as $c_{s,j}$ to denote that it is a pore-scale quantity. On the other hand, the homogenized electrode mass transport equation is derived from Fick's law of diffusion without making any assumption about the particle shape. The concentration term of the homogenized model is a quantity that is averaged over the unit cell.

In the P2D model, the term $D_{s,j}$ represents the pore-scale diffusion coefficient, whereas in the homogenized equation, $\mathbf{D}_{s,j}^{eff}$ represents the effective diffusion tensor. It is obtained by resolving a closure variable, $\chi^s(\mathbf{y})$, in the electrode phase of the unit cell. The electrode closure variable has zero mean, $\langle \chi^s \rangle = 0$, and is determined by resolving the following system of equations [7]:

$$\begin{aligned} \nabla_{\mathbf{y}} \cdot [D_{s,j}(\nabla_{\mathbf{y}}\chi^s + \mathbf{I})] &= 0, & \mathbf{y} \in \mathcal{S}, \\ \mathbf{n}_s \cdot [D_{s,j}(\nabla_{\mathbf{y}}\chi^s + \mathbf{I})] &= 0, & \mathbf{y} \in \Gamma. \end{aligned} \quad (1)$$

\mathbf{y} is a fast space variable in the unit cell Y , $\mathbf{y} \in Y$, and is defined as $\mathbf{y} = \varepsilon^{-1}\mathbf{x}$, where \mathbf{x} is the variable in the macroscale domain [7]. \mathbf{n}_s is a unit normal vector, \mathbf{I} is the identity matrix, \mathcal{S} represents the electrode domain of the unit cell, and Γ represents the interface separating the electrode and electrolyte phases in the unit cell. $D_{s,j}$ is the pore-scale electrode diffusion coefficient and is assumed to be constant, whereas $\mathbf{D}_{s,j}^{eff}$ is obtained by taking the volume average of the term $D_{s,j}(\mathbf{I} + \nabla_{\mathbf{y}}\chi^s)$ in the electrode of the unit cell.

In the P2D model, the pore-scale electrode mass transport equation is used in conjunction with macroscale equations of transport in the electrolyte phase. The justification for this combined implementation of equations at different length scales has not been adequately addressed. On the other hand, the homogenization technique provides a good framework to demonstrate that the electrode phase is always subjected to mass transport limitations. In [7], the applicability conditions in the electrode phase revealed a lack of scale-separation between the *pore* and *macro* scales for different cathode materials. Due to the slow dynamics of lithium diffusion in the electrodes, the continuum description was invalidated. In such cases, either full pore-scale or fully coupled micro-macroscopic equations of mass transport are necessary for accurate modeling of active material transport.

| P2D Model | Homogenized Model |
|---|--|
| Electrode Mass Transport Equation | |
| $\frac{\partial c_{s,j}(x,r,t)}{\partial t} = \frac{D_{s,j}}{r^2} \left(r^2 \frac{\partial c_{s,j}(x,r,t)}{\partial r} \right), \quad j = (n,p)$ | $\frac{\partial \bar{c}_{s,j}}{\partial t} = \nabla \cdot [\mathbf{D}_{s,j}^{eff} \nabla \bar{c}_{s,j}] - \frac{1}{F} J_{Li,j}, \quad j = (n,p)$ |
| Electrolyte Mass Transport Equation | |
| $\eta_{e,j} \frac{\partial \bar{c}_{e,j}(x,t)}{\partial t} = \frac{\partial}{\partial x} \left(D_{e,j}^{eff} \frac{\partial \bar{c}_{e,j}(x,t)}{\partial x} \right) + \frac{(1-t_+)}{F} J_{Li,j}(x,t), \quad j = (n,s,p)$ | $\eta_{e,j} \frac{\partial \bar{c}_{e,j}}{\partial t} = \nabla \cdot \left[\left\{ \mathbf{D}_{e,j}^{eff} + \frac{RT\lambda t_+^2}{F^2 \bar{c}_{e,j}} \mathbf{K}_{e,j}^{eff} \right\} \nabla \bar{c}_{e,j} \right] + \frac{1}{F} J_{Li,j}, \quad j = (n,s,p)$ |
| Electrode Charge Transport Equation | |
| $K_{s,j}^{eff} \frac{\partial^2 \bar{\phi}_{s,j}(x,t)}{\partial x^2} = J_{Li,j}(x,t), \quad j = (n,p)$ | $\nabla \cdot [\mathbf{K}_{s,j}^{eff} \nabla \bar{\phi}_{s,j}] = J_{Li,j}, \quad j = (n,p)$ |
| Electrolyte Charge Transport Equation | |
| $-K_{e,j}^{eff} \frac{\partial^2 \bar{\phi}_{e,j}(x,t)}{\partial x^2} - \frac{2K_{e,j}^{eff}(x,t)RT(1-t_+)}{F} \frac{\partial^2 \ln \bar{c}_{e,j}}{\partial x^2} = J_{Li,j}(x,t), \quad j = (n,s,p)$ | $\nabla \cdot \left[\left\{ \frac{RT\lambda t_+}{F \bar{c}_{e,j}} \mathbf{K}_{e,j}^{eff} \right\} \nabla \bar{c}_{e,j} + \mathbf{K}_{e,j}^{eff} \nabla \bar{\phi}_{e,j} \right] = -J_{Li,j}, \quad j = (n,s,p)$ |
| Intercalation Current Density | |
| $J_{Li,j}(x,t) = a_j k_j \sqrt{c_{s,surf,j} \cdot (c_{s,max,j} - c_{s,surf,j})} \cdot \sqrt{\bar{c}_{e,j}(x,t)} \cdot 2 \sinh \left[\frac{0.5F}{RT} (\bar{\phi}_{s,j} - \bar{\phi}_{e,j} - U_{0,j}) \right], \quad j = (n,p)$ $J_{Li,s}(x,t) = 0$ | $J_{Li,j} = \frac{\varepsilon_j^{-1} \mathcal{K}_j^* \eta_{e,j}}{L_j} \cdot k_j \cdot \sqrt{\bar{c}_{e,j} \cdot \bar{c}_{s,j}} \cdot \left(1 - \frac{\bar{c}_{s,j}}{c_{s,max,j}} \right) \cdot \sinh \left(\frac{F}{2RT} [\bar{\phi}_{s,j} - \bar{\phi}_{e,j} - U_{0,j}] \right), \quad j = (n,p)$ $J_{Li,s} = 0$, because the separator does not contain any active particles |

TABLE I: Transport equations of the homogenized model to describe lithium-ion transport dynamics.

B. Mass transport in the electrolyte

The electrolyte phase lithium-ion transport equation is obtained using the concentrated solution theory. The difference between the P2D and the homogenized model equations can be summarized as follows:

- 1) The P2D model considers the effect of only diffusion in electrolyte mass balance and considers 1-D transport, whereas the homogenized mass transport equation in the electrolyte phase considers the effect of both diffusion and electromigration in multiple dimensions.
- 2) The P2D model approximates effective diffusion and conductivity coefficients based on the asymmetrical Bruggeman effective-medium model [16], also known as the Bruggeman theory. The effective diffusion coefficient is mathematically represented in the P2D model as [17]:

$$D_{e,j}^{eff} = D_{e,j} \cdot \eta_{e,j}^{brugg}, \quad (2)$$

where *brugg* is the Bruggeman exponent, and is typically considered to be equal to 1.5 for perfectly spherical particles [17]. On the other hand, the effective diffusion and conductivity coefficients of the homogenized model, $\mathbf{D}_{e,j}^{eff}$ and $\mathbf{K}_{e,j}^{eff}$, are obtained by taking the volume average of the terms $D_{e,j}(\mathbf{I} + \nabla_{\mathbf{y}} \chi^e)$ and $K_{e,j}(\mathbf{I} + \nabla_{\mathbf{y}} \chi^e)$ in the electrolyte phase of the unit cell. $D_{e,j}$ and $K_{e,j}$ are the pore-scale diffusion and conductivity coefficients respectively, and are assumed constant. The electrolyte closure variable, $\chi^e(\mathbf{y})$, has zero mean, $\langle \chi^e \rangle = 0$, and is defined as the solution to

the local pore-scale problem [7]:

$$\begin{aligned} \nabla_{\mathbf{y}} \cdot (\nabla_{\mathbf{y}} \chi^e + \mathbf{I}) &= 0, & \mathbf{y} \in \mathcal{B}, \\ \mathbf{n}_e \cdot (\nabla_{\mathbf{y}} \chi^e + \mathbf{I}) &= 0, & \mathbf{y} \in \Gamma. \end{aligned} \quad (3)$$

In (3), \mathcal{B} represents the electrode domain of the unit cell. The Bruggeman approximation works well only for the case of dilute electrolyte solutions. Du *et. al.* [13] report significant deviation of the effective transport coefficients from the Bruggeman approximation when experiments are compared to pore-scale simulations of battery dynamics.

C. Charge transport in the electrode

The solid phase lithium-ion potential is obtained using the charge conservation equation described by Ohm's law, and modeled as a 1-D transport equation in the P2D model. The effective electrode conductivity in the P2D model is expressed in terms of the electrode porosity as [17]:

$$K_{s,j}^{eff} = K_{s,j} \cdot \eta_{s,j}^{brugg}, \quad (4)$$

On the other hand, in the homogenized model, $\mathbf{K}_{s,j}^{eff}$ is the effective solid-phase conductivity parameter, obtained by the taking the volume average of the term $K_{s,j}(\nabla_{\mathbf{y}} \chi^s + \mathbf{I})$ in the electrode of the unit cell. $K_{s,j}$ is the pore-scale conductivity coefficient and is assumed to be constant. The closure variable $\chi^s(\mathbf{y})$ is obtained by resolving the unit cell problem [7]:

$$\begin{aligned} \nabla_{\mathbf{y}} \cdot [K_{s,j}(\nabla_{\mathbf{y}} \chi + \mathbf{I})] &= 0, & \mathbf{y} \in \mathcal{S}, \\ \mathbf{n}_s \cdot [K_{s,j}(\nabla_{\mathbf{y}} \chi + \mathbf{I})] &= 0, & \mathbf{y} \in \Gamma. \end{aligned} \quad (5)$$

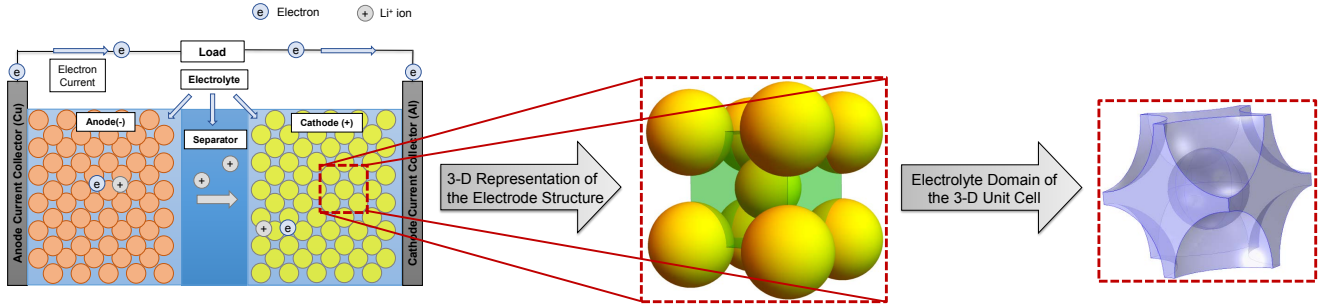


Fig. 1: Schematic representation of a lithium-ion battery (left), the corresponding 3-D electrode microstructure (middle), and the representative unit cell in which the closure variable is resolved (right).

D. Charge transport in the electrolyte

The equation for the electrolyte phase lithium-ion charge transport is obtained by combining Kirchhoff's law with Ohm's law, and is modeled as a 1-D transport equation in the P2D model. The effective electrolyte conductivity is mathematically represented using the Bruggeman theory as [17]:

$$K_{e,j}^{eff} = K_{e,j} \cdot \eta_{e,j}^{brugg}, \quad (6)$$

where the Bruggeman coefficient is assumed to be equal to 1.5 [17]. On the other hand, the effective electrolyte conductivity $K_{e,j}^{eff}$ in (3) is obtained by resolving the closure variable $\chi^e(\mathbf{y})$ in the electrolyte domain of the unit cell.

E. Remarks

- 1) The homogenization technique, represents pore-scale quantities as an asymptotic series in powers of the scale separation parameter ε^1 . On the other hand, the P2D model approximates the pore-scale PNP equations such that only the zeroth order terms of an asymptotic series expansion are accounted for [2].
- 2) The P2D model has an order of accuracy of ε and must rely on significantly small ratio of length scales between the micro and macro media [2], while the homogenization model has an accuracy of the order of ε^2 [7].
- 3) The P2D model accounts for only spherically shaped active particle in the determination of the effective parameters. As evidenced by the scanning electron microscope images of the structure of lithium cobalt oxide cathode and graphite anode [17], the homogenized electrode material balance equation is better suited for resolving concentration dynamics in these electrodes.
- 4) The homogenization technique provides a more robust approach to determine the effective transport parameters when the analytical expressions, such as the Bruggeman relationship, are invalidated.

¹The scale separation parameter ε is defined as the ratio of the characteristic length scale l of the unit cell Y , and the characteristic length scale L of the porous electrode: $\varepsilon \equiv \frac{l}{L}$. For porous battery electrodes, L is typically of the order of the thickness of the electrode under consideration. [7]

III. SIGNIFICANCE OF THE CLOSURE VARIABLE

The effective diffusion and conductivity parameters of the homogenized model are resolved by a multiscale approach where a pore-scale closure problem is solved at the unit cell of the electrodes. This approach allows the incorporation of the microstructural grain distribution in order to estimate the effective parameters. Garcia *et. al.* [18] and Tartakovsky *et. al.* [19] have demonstrated the impact of the underlying electrode morphology on the performance of electrochemical energy storage devices and elucidate the need for optimizing their geometrical configuration. The topology of the porous electrodes is critical for the estimation of their effective material transport properties. The advantage of the closure variable is its ability to assess material performance for different topological structures on the pore-scale. Such information cannot be captured by standard techniques such as the Bruggeman approximation.

IV. SOLUTION OF THE CLOSURE PROBLEM AND DETERMINATION OF THE EFFECTIVE PARAMETERS

The closure variable accounts of the impact of the pore-scale structure and can be determined using offline calculations. As a result, the closure problem can be resolved as a pre-processing step and the effective parameter values can be directly used in the homogenized model equations. Numerical simulation for the closure problem is performed in a cubic unit cell containing spherical active particles using the computational fluid dynamics solver OpenFOAM [14].

Fig. 1 shows the schematic representation of a lithium-ion battery. In this study, we select spherical active particles to make a direct comparison with the effective parameter values using Bruggeman theory. The cubic unit cell of the electrode is of dimensions $\{10.94\mu\text{m}, 10.94\mu\text{m}, 10.94\mu\text{m}\}$, consists of spherical particles of radius $5\mu\text{m}$ with centers at each corner of the unit cell, and a spherical particle at the center of the unit cell. This geometrical configuration results in an electrolyte volume fraction of 0.4. Since the closure variable $\chi^e(\mathbf{y})$ is solved in the fast variable \mathbf{y} , the size of the unit cell is $\{1,1,1\}$. The dimensions of the spherical particles within the unit cell are also normalized, and they have a dimensionless radius of 0.46. Fig. 1 also illustrates

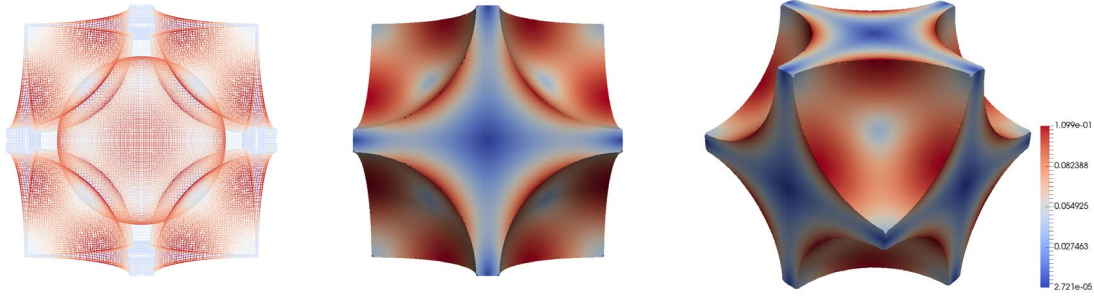


Fig. 2: Schematic representation of the mesh used to solve for closure variable (left). The 2-D (middle) and 3-D (right) plots represent the magnitude of the resolved closure variable. The porosity of the unit cell considered in this study is equal to 0.40.

the spherical particle configuration in the unit cell and the domain of the electrolyte in a representative unit cell of the electrode.

The closure variable, $\chi^e(\mathbf{y})$, defined in (3), is solved in the electrolyte domain through *laplacianFoam*. The mesh in which the finite volume analysis is performed is prepared with *snappyHexMesh*, with standard sets of parameters, and is shown in Fig. 2. The discretized equations are solved using standard linear solvers. The boundary conditions for the closure problem are implemented through the extension *groovyBC* of the OpenFOAM library *swak4Foam*. The boundary condition for the closure variable is imposed at the interface separating the spherical active particles and the electrolyte. Fig. 2, represents the distribution of the resolved closure variable in the electrolyte domain. The superficial average values of the x-, y-, and z-components of $\chi^e(\mathbf{y})$ are respectively $6.43e-6$, $6.40e-6$, and $6.38e-6$. The results obtained are consistent with the definition of the closure variable, since they satisfy the zero mean criteria, $\langle \chi^e \rangle = \mathbf{0}$, with a numerical accuracy in the unit cell.

The pore-scale diffusion coefficient, $D_{e,j}$, and the pore-scale conductivity coefficient, $K_{e,j}$, are assumed to be constant. As a result, the effective diffusion tensor, $\mathbf{D}_{e,j}^{eff}$ and the effective conductivity tensor, $\mathbf{K}_{e,j}^{eff}$, can be determined by computing the superficial average of the tensor $(\mathbf{I} + \nabla_{\mathbf{y}}\chi^e)$. The superficial average of this tensor results in the following matrix:

$$\begin{bmatrix} 0.299 & -6.63e-10 & -3.62e-7 \\ -4.34e-10 & 0.299 & -1.36e-10 \\ -2.87e-7 & 3e-10 & 0.299 \end{bmatrix} \quad (7)$$

The tensor in (7) is essentially diagonal, with negligible off-diagonal components. We also note that the tensor is isotropic, due to the symmetric nature of the unit cell in which the closure variable was resolved. As a result, the tensor can be expressed as $0.299 \mathbf{I}$, where \mathbf{I} is the identity matrix. We compare the effective diffusion and conductivity parameters obtained from the closure variable with the parameter values obtained using the Bruggeman theory. The values of the parameters, $D_{e,p} = 3.94e-11 \text{ m}^2\text{s}^{-1}$, and $K_{e,p} = 0.192 \text{ S}^{-1}\text{m}^{-1}$ are obtained from literature [20]. The effective transport parameters is obtained by the product of

the pore-scale transport coefficients with the tensor $0.299 \mathbf{I}$:

$$\begin{aligned} \mathbf{D}_{e,j}^{eff} &= (0.299 \cdot 3.94e-11) \mathbf{I} \text{ m}^2\text{s}^{-1} \\ &= 1.18e-11 \mathbf{I} \text{ m}^2\text{s}^{-1}, \\ \mathbf{K}_{e,j}^{eff} &= (0.299 \cdot 0.192) \mathbf{I} \text{ S}^{-1}\text{m}^{-1} \\ &= 0.060 \mathbf{I} \text{ S}^{-1}\text{m}^{-1} \end{aligned} \quad (8)$$

The effective transport parameters determined by the Bruggeman theory are obtained by using equations (2) and (4) respectively:

$$\begin{aligned} D_{e,j}^{eff} &= 3.94e-11 \cdot (0.4)^{1.5} = 0.99e-11 \text{ m}^2\text{s}^{-1}, \\ K_{e,j}^{eff} &= 0.192 \cdot (0.4)^{1.5} = 0.048 \text{ S}^{-1}\text{m}^{-1} \end{aligned} \quad (9)$$

Comparison with an isotropic diagonal element of the closure-based effective parameters indicates that the Bruggeman theory underpredicts the effective parameter values in the electrolyte medium. This can be observed by comparing the results shown in (8) and (9). This analysis can be extended in a similar manner to determine the effective transport parameters in the anode and the separator. The closure problem was resolved for the following values of porosity: $\{0.30, 0.40, 0.48, 0.56, 0.62\}$ using a unit cell configuration similar to that shown in Fig. 1. In each case, the values of effective diffusion and conductivity were calculated for the closure and the Bruggeman approach. The results of this study are summarized in Fig. 3, where the diagonal element of the effective parameter from the closure approach and the effective parameter value from the Bruggeman approach are plotted as a function of the porosity. Both approaches indicate that the effective transport parameters increase with porosity, with the closure-based approach resulting in higher effective parameter values. The results indicate that the geometry of the unit cell strongly influences the effective transport parameters. For the spherical particle geometry, which is one of the simplest structures that can be considered, the Bruggeman theory still underpredicted the effective parameter values by about 20% for a unit cell porosity of 0.40. Such influence of the electrode geometry on the effective parameters could be even more pronounced for complex non-spherical active particles.

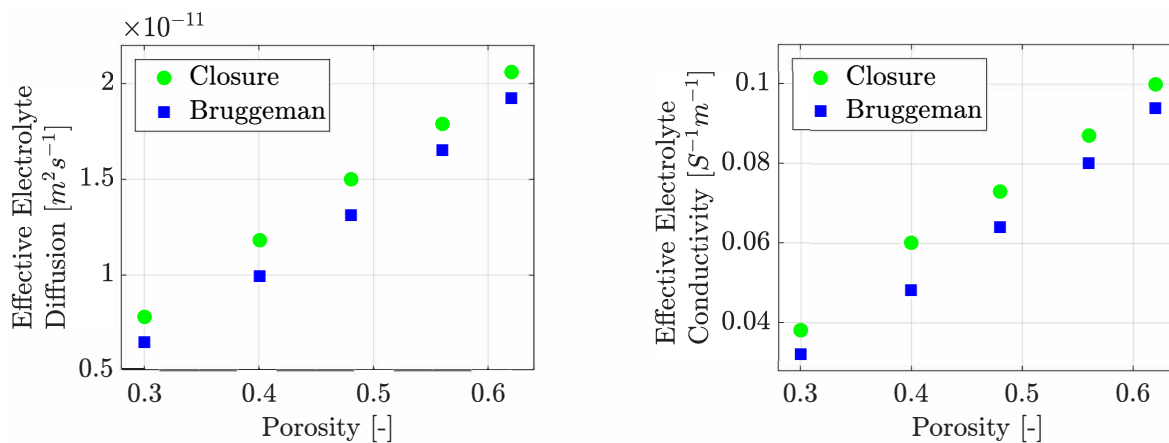


Fig. 3: Comparison of the effective electrolyte diffusion (left) and effective electrolyte conductivity (right) calculated using the closure and the Bruggeman approach. Effective transport properties increase with porosity, and higher effective parameter values are obtained using the closure approach.

V. CONCLUSIONS

In this paper, we presented a new class of macroscopic mass and charge transport equations for lithium-ion battery dynamics, which were rigorously derived using the homogenization technique. We presented a detailed comparison analysis of our model equations with respect to the extensively used P2D model, outlining factors that indicate a higher predictive ability of the proposed model. For the very first time, a finite volume approach is presented using OpenFOAM to resolve the unit-cell closure problem for porous battery electrodes. The closure variable results are integrated in the homogenized model equations through the effective transport parameters. We envision these results to have the following implications to the battery system community: **a)** the closure-approach will enable more accurate modeling capability of lithium-ion transport in non-spherical active particle electrodes, thanks to the solution of the closure problem, and **b)** the proposed enhanced modeling framework will provide benefits from a performance standpoint through accurate prediction of battery dynamics for higher C-rates of operation, wider envelope of operating temperature conditions, and cycle life aging. Ultimately, this work will pave the way for developing strategies to prolong battery life through accurate modeling and control.

REFERENCES

- [1] M. Doyle, T. F. Fuller, and J. Newman, "Modeling of Galvanostatic Charge and Discharge of the Lithium/Polymer/Insertion Cell," *J. Electrochem. Soc.*, vol. 140, no. 6, pp. 1526–1533, 1993.
- [2] F. Ciucci and W. Lai, "Derivation of Micro/Macro Lithium Battery Models from Homogenization," *Transp. Porous Media*, vol. 88, no. 2, pp. 249–270, 2011.
- [3] G. H. Kim, K. Smith, K. J. Lee, S. Santhanagopalan, and A. Pesaran, "Multi-Domain Modeling of Lithium-Ion Batteries Encompassing Multi-Physics in Varied Length Scales," *J. Electrochem. Soc.*, vol. 158, no. 8, pp. A955–A969, 2011.
- [4] R. E. Garcia and Y.-M. Chiang, "Spatially resolved modeling of microstructurally complex battery architectures," *J. Electrochem. Soc.*, vol. 154, no. 9, pp. A856–A864, 2007.
- [5] R. E. Gerver, *3D thermal-electrochemical lithium-ion battery computational modeling*. University of Texas Libraries, 2009.
- [6] X. Zhang, *Multiscale modeling of Li-ion cells: mechanics, heat generation and electrochemical kinetics*. PhD thesis, The University of Michigan, 2009.
- [7] H. Arunachalam, S. Onori, and I. Battiato, "On Veracity of Macroscopic Lithium-Ion Battery Models," *J. Electrochem. Soc.*, vol. 162, no. 10, pp. A1940–A1951, 2015.
- [8] H. Arunachalam, S. Onori, and I. Battiato, "Temperature-dependent multiscale-dynamics in Lithium-ion battery electrochemical models," in *Proceedings of the 2015 American Control Conference*, pp. 305–310, 2015.
- [9] D. Kehrwald, P. R. Shearing, N. P. Brandon, P. K. Sinha, and S. J. Harris, "Local tortuosity inhomogeneities in a lithium battery composite electrode," *J. Electrochem. Soc.*, vol. 158, no. 12, pp. A1393–A1399, 2011.
- [10] M. Guo, G. Sikha, and R. E. White, "Single-particle model for a lithium-ion cell: Thermal behavior," *J. Electrochem. Soc.*, vol. 158, no. 2, pp. A122–A132, 2011.
- [11] L. Cai and R. E. White, "Reduction of Model Order Based on Proper Orthogonal Decomposition for Lithium-Ion Battery Simulations," *J. Electrochem. Soc.*, vol. 156, no. 3, pp. A154–A161, 2009.
- [12] S. J. Moura, N. A. Chaturvedi, and M. Krstić, "Constraint management in li-ion batteries: A modified reference governor approach," in *American Control Conference (ACC), 2013*, pp. 5332–5337, IEEE, 2013.
- [13] W. Du, N. Xue, W. Shyy, and J. R. R. A. Martins, "A Surrogate-Based Multi-Scale Model for Mass Transport and Electrochemical Kinetics in Lithium-Ion Battery Electrodes," *J. Electrochem. Soc.*, vol. 161, no. 8, pp. E3086–E3096, 2014.
- [14] "The openFOAM Foundation." <http://www.openfoam.org/>. Accessed: 2017.
- [15] T.-S. Dao, C. P. Vyasayani, and J. McPhee, "Simplification and order reduction of lithium-ion battery model based on porous-electrode theory," *J. Power Sources*, vol. 198, pp. 329–337, 2012.
- [16] D. S. McLachlan, J. H. Hwang, and T. O. Mason, "Evaluating Dielectric Impedance Spectra using Effective Media Theories," *J. Electroceram.*, vol. 5, no. 1, pp. 37–51, 2000.
- [17] M. Ebner, D. W. Chung, R. E. Garcia, and V. Wood, "Tortuosity Anisotropy in Lithium-Ion Battery Electrodes," *Advanced Energy Materials*, vol. 4, no. 5, 2014.
- [18] D.-W. Chung, M. Ebner, D. R. Ely, V. Wood, and R. E. Garcia, "Validity of the Bruggeman relation for porous electrodes," *Modelling and Simulation in Materials Science and Engineering*, vol. 21, no. 7, p. 074009, 2013.
- [19] X. Zhang and D. M. Tartakovsky, "Effective Ion Diffusion in Charged Nanoporous Materials," *J. Electrochem. Soc.*, vol. 164, no. 4, pp. E53–E61, 2017.
- [20] L. Zhang, L. Wang, G. Hinds, C. Lyu, J. Zheng, and J. Li, "Multi-objective optimization of lithium-ion battery model using genetic algorithm approach," *J. Power Sources*, vol. 270, pp. 367–378, 2014.